



# Immunological characterization of two types of ionocytes in the inner ear epithelium of Pacific Chub Mackerel (*Scomber japonicus*)

Garfield T. Kwan<sup>1</sup> · Taylor R. Smith<sup>1</sup> · Martin Tresguerres<sup>1</sup>

Received: 20 January 2020 / Revised: 20 January 2020 / Accepted: 30 March 2020  
© Springer-Verlag GmbH Germany, part of Springer Nature 2020

## Abstract

The inner ear is essential for maintaining balance and hearing predator and prey in the environment. Each inner ear contains three  $\text{CaCO}_3$  otolith polycrystals, which are calcified within an alkaline,  $\text{K}^+$ -rich endolymph secreted by the surrounding epithelium. However, the underlying cellular mechanisms are poorly understood, especially in marine fish. Here, we investigated the presence and cellular localization of several ion-transporting proteins within the saccular epithelium of the Pacific Chub Mackerel (*Scomber japonicus*). Western blotting revealed the presence of  $\text{Na}^+/\text{K}^+$ -ATPase (NKA), carbonic anhydrase (CA),  $\text{Na}^+/\text{K}^+/\text{2Cl}^-$ -co-transporter (NKCC), vacuolar-type  $\text{H}^+$ -ATPase (VHA), plasma membrane  $\text{Ca}^{2+}$  ATPase (PMCA), and soluble adenylyl cyclase (sAC). Immunohistochemistry analysis identified two distinct ionocytes types in the saccular epithelium: Type-I ionocytes were mitochondrion-rich and abundantly expressed NKA and NKCC in their basolateral membrane, indicating a role in secreting  $\text{K}^+$  into the endolymph. On the other hand, Type-II ionocytes were enriched in cytoplasmic CA and VHA, suggesting they help transport  $\text{HCO}_3^-$  into the endolymph and remove  $\text{H}^+$ . In addition, both types of ionocytes expressed cytoplasmic PMCA, which is likely involved in  $\text{Ca}^{2+}$  transport and homeostasis, as well as sAC, an evolutionary conserved acid–base sensing enzyme that regulates epithelial ion transport. Furthermore, CA, VHA, and sAC were also expressed within the capillaries that supply blood to the meshwork area, suggesting additional mechanisms that contribute to otolith calcification. This information improves our knowledge about the cellular mechanisms responsible for endolymph ion regulation and otolith formation, and can help understand responses to environmental stressors such as ocean acidification.

**Keywords** ATPase · Biomineralization · Calcification · Ocean acidification · Otolith · Soluble adenylyl cyclase

## Introduction

The inner ear senses gravity and sound waves, which is essential for maintaining balance and hearing predator and prey in the environment (Dijkgraaf 1960; Furukawa and Ishii 1967; reviewed in Ladich and Schulz-Mirbach 2016). Enclosed within each inner ear are the sagittal, lapilli, and asterisci otoliths, which are composed of a protein matrix and calcium carbonate ( $\text{CaCO}_3$ ). The higher density of the otolith compared to the inner ear fluid (“endolymph”) results

in differential inertia that stimulates the adjacent sensory hair cells, which the brain interprets as soundwaves or movement.

Being the largest of the three otoliths, the sagitta and its surrounding saccular epithelium have been most extensively studied. The saccular epithelium has been previously characterized as the macula, meshwork, patches, and intermediate areas (Mayer-Gostan et al. 1997; Pisam et al. 1998). The macula contains the sensory hair cells that detect otolith vibration and movement. This area is flanked by the meshwork area, which contains large ion-transporting cells (“ionocytes”). The patches area is positioned directly across from the macula and contains patches of smaller ionocytes. The intermediate area is largely devoid of ionocytes, but does contain some ionocytes in the area bordering the meshwork area and smaller ionocytes bordering the patches area. Each otolith is calcified within an alkaline,  $\text{K}^+$ -rich

---

Communicated by Bernd Pelster.

✉ Martin Tresguerres  
mtresguerres@ucsd.edu

<sup>1</sup> Marine Biology Research Division, Scripps Institution of Oceanography, University of California San Diego, La Jolla, USA

endolymph secreted by its respective saccule, utricle and lagena inner ear epithelium.

In the Rainbow Trout (*Oncorhynchus mykiss*), the endolymph has a pH of  $\sim 8$ ,  $\sim 30$  mmol of  $\text{HCO}_3^-$ ,  $\sim 124$  mmol of  $\text{K}^+$ ,  $\sim 90$  mmol of  $\text{Na}^+$ , and  $\sim 1.1$  mmol of  $\text{Ca}^{2+}$  (Payan et al. 1997). When compared to its blood plasma, the endolymph is roughly 0.8 pH unit higher, has twice as much  $\text{HCO}_3^-$ ,  $\sim 40$ -fold higher  $\text{K}^+$ , half as much  $\text{Na}^+$ , and twice as much  $\text{Ca}^{2+}$  (Payan et al. 1997). This dramatic differences between the endolymph and blood plasma are thought to be attributed to the surrounding ionocytes' activity. To date, two different types of ionocytes have been characterized: one is mitochondrion-rich (MR), has well-developed basolateral membrane infoldings (Mayer-Gostan et al. 1997), and abundantly expresses  $\text{Na}^+/\text{K}^+$ -ATPase (NKA) (Takagi 1997), whereas the other one has abundant cytoplasmic carbonic anhydrase (CA) (Tohse et al. 2004, 2006). The NKA-rich ionocytes are proposed to be responsible for transporting  $\text{K}^+$  (Payan et al. 1999),  $\text{Ca}^{2+}$  (Mugiya and Yoshida 1995) and removing  $\text{H}^+$  (Payan et al. 1997) from the endolymph, whereas the CA-rich ionocytes are thought to transport  $\text{HCO}_3^-$  into the endolymph (Tohse and Mugiya 2001; reviewed in Payan et al. 2004). These models would imply the NKA-rich ionocytes should have different ion-transporting proteins than the CA-rich ionocytes.

Moreover, the endolymph's composition is not homogeneous (Payan et al. 1999; Borelli et al. 2003). The proximal endolymph, which is located between the otolith and the macula and meshwork area, has lower  $[\text{K}^+]$  and total  $\text{CO}_2$  compared to the distal endolymph, which is located between the other side of the otolith and the intermediate and patches area (Payan et al. 1999). Though  $[\text{Ca}^{2+}]$  does not differ between the proximal and distal endolymph (Payan et al. 1999; Borelli et al. 2003), the proximal endolymph has a threefold higher concentration of glycoprotein (Payan et al. 1999), which may chelate  $\text{Ca}^{2+}$  and catalyze aragonite crystallization (Murayama et al. 2002; Ibsch et al. 2004). Correspondingly, the otolith's proximal surface calcifies faster than the distal surface (Payan et al. 1999; Borelli et al. 2003; Beier et al. 2006). And although it was not directly measured, it was further hypothesized that the pH in the proximal endolymph is lower than the distal endolymph as increased otolith calcification would locally increase  $[\text{H}^+]$  (Payan et al. 1999). This heterogeneity of the proximal and distal endolymph was proposed to be the result of differential ion transporting activity of meshwork and patches ionocytes. Under this model, the larger NKA-rich ionocytes in the meshwork area remove  $\text{K}^+$  from the proximal endolymph, whereas the smaller NKA-rich ionocytes in the patches area secrete  $\text{K}^+$  and absorb  $\text{H}^+$  at the distal endolymph (Payan et al. 1999; Allemand et al. 2008). Similarly, other studies speculated that the larger meshwork CA-rich ionocytes remove  $\text{H}^+$  from the proximal endolymph (Tohse et al. 2006). These

models imply that NKA-rich and CA-rich ionocytes in the meshwork area should express different proteins than their counterparts in the patches area.

Although many other proteins are known to be expressed in the fish inner ear, to our knowledge NKA and CA are the only two ion-transporting proteins established to be specifically present in ionocytes. Basolateral  $\text{Na}^+/\text{K}^+/\text{2Cl}^-$ -co-transporter (NKCC1; *slc12a2*, NKCC1) is expressed in their developing inner ear of Zebrafish (*Danio rerio*) larvae (Abbas and Whitfield 2009). Although the lack of endolymph accumulation upon NKCC1 genetic disruption indicated a role in  $\text{K}^+$  and fluid secretion, the specific cell type, where this protein is expressed was not established. Another study detected abundant intracellular acidic compartments in a subset of trout inner ear epithelial cells and hypothesized it indicated removal of  $\text{H}^+$  from the endolymph by V-type  $\text{H}^+$ -ATPase (VHA) (Mayer-Gostan et al. 1997). However, a subsequent study did not find VHA in Zebrafish inner ear ionocytes, and instead reported VHA expression within inner ear sensory hair cells and proposed it acidified the proximal endolymph to retard otolith calcification and maintain distance with the hair cells (Shiao et al. 2005). The plasma membrane  $\text{Ca}^{2+}$ -ATPase (PMCA; *atp2b1a*) was proposed to be expressed in MR-ionocytes and to transport  $\text{Ca}^{2+}$  for otolith calcification (Mugiya and Yoshida, 1995; Payan et al. 2002). In situ hybridization showed the presence of PMCA mRNA in some epithelial cells surrounding the sensory macula of the developing inner ear of Zebrafish larvae; however, attempts to immunolocalize the protein were unsuccessful in both larval and adult tissues and thus remain unknown whether PMCA is expressed in ionocytes (Cruz et al. 2009). More recently, a comprehensive transcriptomic and proteomic study concluded NKA, CA, VHA, and PMCA are expressed in the inner ear of black bream (*Acanthopagrus butcheri*) (Thomas et al. 2019). However, those analyses were conducted on samples that contained both inner ear and brain tissue, and thus did not provide insights about protein expression in specific cells. In summary, there are many excellent studies about the ion-transporting proteins involved in otolith calcification, but their use of different fish species, life stages, and techniques greatly complicates attempts to synthesize the available information into a single model describing the ion transporting mechanisms that maintain the distinctive endolymph composition necessary for proper inner ear function.

Although the cellular mechanisms underlying otolith calcification are not completely understood, it is clear that they activities are sensitive to acid–base conditions (reviewed in Allemand et al. 2008). Indeed, diurnal fluctuations in plasma  $[\text{HCO}_3^-]$  is one of the underlying causes of the otolith's characteristic concentric rings (Tohse and Mugiya, 2008) used to estimate age and growth in stock assessment studies (Pannella 1971; Campana and Neilson, 1985). And

more recently, exposure to ocean acidification conditions has been reported to induce increased otolith size and density in multiple fish species (Checkley et al. 2009; Bignami et al. 2013; Maneja et al. 2013; Munday et al. 2011; Pimentel et al. 2014; Schade et al. 2014; Shen et al. 2016), which has been linked to plasma  $[\text{HCO}_3^-]$  accumulation resulting from blood acid–base regulation [c.f. (Esbaugh et al. 2012, 2016)]. One possibility is that otolith overgrowth is the direct result of increased transport of plasma  $[\text{HCO}_3^-]$  into the endolymph. However, increased otolith calcification rate also requires increased secretion of  $\text{Ca}^{2+}$  and glycoprotein into the endolymph, and increased  $\text{H}^+$  removal. With this in mind, we explored whether the soluble adenylyl cyclase (sAC, *adcy10*) is expressed within inner ear epithelial ionocytes. This evolutionary conserved acid–base sensing enzyme is stimulated by  $\text{HCO}_3^-$  to produce cyclic adenosine monophosphate (cAMP), a messenger molecule that can regulate multiple cellular processes via protein kinase A mediated phosphorylation on target proteins (reviewed in Tresguerres et al. 2010a; Tresguerres 2014).

The goal of the current study was to determine how many types of ionocytes are present in the inner ear epithelium of a single species, the Pacific Chub Mackerel (*Scomber japonicus*, Houttuyn, 1782). To this end, we performed thorough immunohistochemical analyses using specific antibodies against NKA, CA, NKCC, VHA, PMCA, and sAC. Unexpectedly, we also detected high abundance of some of these proteins in the cells that form the arterioles that supply blood to the meshwork area. The resulting model about the ion-transporting and regulatory mechanisms underlying endolymph's unique composition improves our understanding about how otoliths are calcified, and will inform subsequent experimental studies to determine if and how they might be affected during environmental stress.

## Methods

### Tissue sampling and preparation

Pacific Chub Mackerel were caught by hook and line off the Scripps pier in San Diego, United States (standard length =  $15.3 \pm 0.3$  cm; weight =  $26.9 \pm 2.2$  g;  $n = 19$ ). In accordance to protocol S10320 of the University of California, San Diego Institutional of Animal Care and Use Committee, fish were euthanized by spinal pithing and its inner ear tissue dissected. Tissue was either flash frozen in liquid nitrogen and stored in  $-80$  °C, or fixed in 4% paraformaldehyde in phosphate buffer saline (PBS) at 4 °C for 8 h, incubated in 50% ethanol for 8 h, and stored in 70% ethanol for immunohistochemistry. Protein integrity was prioritized; therefore, the length and weight of the fish were recorded after dissection.

## Antibodies

Mitochondria were labeled using a mouse monoclonal antibody against human cytochrome *c* oxidase complex IV (MTC02, catalog #: MA5-12,017, Invitrogen, Grand Island, New York, USA); this antibody demonstrates specificity against a broad range of species including coral (Barott et al. 2015b) and shark (Roa et al. 2014). The mouse monoclonal anti-NKA antibody  $\alpha 5$  (Lebovitz et al. 1989) was purchased from the Developmental Studies Hybridoma Bank (DSHB, The University of Iowa, Iowa City, IA, USA). This antibody has been extensively validated in fish and is routinely used to detect NKA in multiple fish tissues (Wilson et al. 2000, 2002; Roa et al. 2014; Roa and Tresguerres 2017; Kwan et al. 2019). In addition, NKA was immunodetected using rabbit polyclonal antibodies against the mammalian NKA  $\alpha$ -subunit (H300, catalog # SC-28800, Santa Cruz Biotechnology, Dallas, USA), which recognize NKA in gills from multiple fish (Roa et al. 2014; Michael et al. 2016; Allmon and Esbaugh, 2017). Rabbit polyclonal antibodies against human CA II were purchased from Rockland Inc., Gilbertsville, USA (catalog #: 100-401-136); these antibodies are routinely used to immunodetect CA from teleost fish [e.g., (Georgalis et al. 2006; Qin et al. 2010)], including in the saccular epithelium of Masu Salmon (*Oncorhynchus masou*) (Tohse et al. 2004). The mouse monoclonal anti-NKCC antibody T4 (Lytle et al. 1995) was obtained from DSHB; and has been widely used to detect NKCC in fish tissues (Tresguerres et al. 2010b; Esbaugh and Cutler 2016), including Zebrafish saccular epithelium (Abbas and Whitfield 2009). VHA was immunodetected using custom-made rabbit polyclonal antibodies against a peptide in the B subunit (epitope: AREEVPGRRGFPGY; GenScript, Piscataway, USA); this peptide is conserved from cnidarians to mammals (Barott et al. 2015a, b), and has been successfully used to immunodetect VHA in elasmobranch tissues (Roa et al. 2014; Roa and Tresguerres 2017). However, T4 can also recognize  $\text{Na}^+/\text{Cl}^-$ -co-transporter (Hiroi et al. 2008; Inokuchi et al. 2008) and should be validated. The mouse monoclonal anti-PMCA antibody 5F10 against human erythrocyte PMCA was purchased from ThermoFisher Scientific, Waltham, USA (catalog #: MA3-914). sAC was immunodetected using custom-made rabbit polyclonal antibodies against a peptide in the first catalytic domain of Rainbow Trout sAC (epitope: LSSKKGYGADDELTR; GenScript). The secondary antibodies were goat anti-mouse IgG-HRP and goat anti-rabbit IgG-HRP conjugate (Bio-Rad, Hercules, CA, USA) for western blot, and goat anti-mouse Alexa Fluor 546, goat anti-rabbit Alexa Fluor 488, and/or goat anti-rabbit Alexa Fluor 555 (Invitrogen, Grand Island, USA) for immunohistochemistry. Each antibody was tested in inner ear samples from at least three different fishes.

## Western blotting

Inner ear tissue was immersed in liquid nitrogen, pulverized in a porcelain grinder, and submerged in an ice-cold, protease inhibiting buffer (250 mmol l<sup>-1</sup> sucrose, 1 mmol l<sup>-1</sup> EDTA, 30 mmol l<sup>-1</sup> Tris, 10 mmol l<sup>-1</sup> benzamidine hydrochloride hydrate, 200 mmol l<sup>-1</sup> phenylmethanesulfonyl fluoride, 1 mol l<sup>-1</sup> dithiothreitol, pH 7.5). Next, debris was removed by low speed centrifugation (3000xg, 10 min, 4 °C). Total protein concentration in the crude homogenate was determined by the Bradford assay (Bradford 1976). Samples were mixed with an equal volume of 90% 2×Laemmli buffer and 10% β-mercaptoethanol, and heated at 70 °C for 5 min. Protein (10 µg per lane) were loaded onto a 7.5% polyacrylamide mini gel (Bio-Rad, Hercules, CA, USA) and ran at 200 V for 40 min, then transferred to a polyvinylidene difluoride (PVDF) membrane using a Trans-Blot SD Semi-Dry Transfer Cell (Bio-Rad). PVDF membranes were then incubated in tris-buffered saline with 1% tween (TBS-T) with milk powder (0.1 g/mL) at room temperature (RT) for 1 h, then incubated with primary antibody (a5: 10.5 ng/ml; H300: 100 ng/ml; CA II antibody: 8 µg/ml; T4: 10.4 ng/ml; VHA *b*-subunit: 1.5 µg/ml; Rainbow Trout sAC: 3 µg/ml; 5F10: diluted 1:10,000 from commercial stock) in blocking buffer at 4 °C overnight. On the following day, PVDF membranes were washed in TBS-T (three times; 10 min each), incubated in the appropriate anti-rabbit or anti-mouse secondary antibodies (1:10,000) at RT for 1 h, and washed again in TBS-T (three times; 10 min each). Bands were made visible through addition of ECL Prime Western Blotting Detection Reagent (GE Healthcare, Waukesha, WI) and imaged and analyzed in a BioRad Universal III Hood using Image Lab software (version 6.0.1; BioRad). Peptide preabsorption with excess peptide (1:5 antibody to peptide ratio; preabsorbed overnight at 4 °C on shaker) was performed to verify antibody specificity.

## Immunostaining

After fixation, samples were immersed in decalcifying solution (NaCl 450 mM, KCL 10 mM, MgCl 58 mM, Hepes 100 mM, EDTA 0.5 M, pH 7.5, changed daily) for 3 days at 4 °C on a shake table to dissolve the otolith. Once the otolith dissolved, samples were incubated overnight in 70% ethanol and dehydrated through a series of increasing ethanol steps (70%, 95%, 100%, 10 min each), SafeClear (three times; 10 min each), warm paraffin (65 °C; three times; 10 min each), before embedding tissue in a paraffin block on an ice pack overnight. The next day, samples were sectioned using a microtome (~ 10 µm thickness) and mounted onto glass slides. After drying overnight, paraffin was removed by incubation in SafeClear (three times; 10 min each), and rehydrated in a series of decreasing ethanol steps (100%,

95%, 70%, 10 min each). To counter native autofluorescence, samples were immersed with sodium borohydride (1 mg/ml) in ice cold PBS (six times; 10 min each). Samples were then washed in PBS + 0.1% tween (PBS-T) at RT for 5 min, incubated in blocking buffer (PBS-T, 0.02% normal goat serum, 0.0002% keyhole limpet hemocyanin) at RT for 1 h, and with the primary antibodies (MTC02: 2 µg/ml; a5: 42 ng/ml; H300: 4 µg/ml; CA II antibody: 160 µg/ml; T4: 104 ng/ml; VHA *b*-subunit: 6 µg/ml; Rainbow Trout sAC: 6 µg/ml; 5F10: diluted 1:500 from commercial stock) in blocking buffer and kept in a humid chamber at RT overnight. On the following day, samples were washed in PBS-T (three times; 10 min each) and incubated with the appropriate anti-rabbit or anti-mouse fluorescent secondary antibodies (1:1,000) and nuclear stain Hoechst 33,342 (5 µg/ml; Invitrogen) at RT for 1 h. Samples were washed in PBS-T (three times; 10 min each), then mounted in Fluoro-gel with Tris (Electron Microscopy Sciences). Samples were examined and imaged on an epifluorescence microscope (Zeiss AxioObserver Z1). Digital images were adjusted, for brightness and contrast, using Zeiss Axiovision software. Some low magnification images were stitched together to provide pictures of the entire saccular epithelium using Helicon Focus 6 (Helicon Soft Ltd., Kharkov, Ukraine). Peptide preabsorption with excess peptide (1:10 antibody to peptide ratio; preabsorbed overnight at 4 °C on shaker) was performed to verify antibody specificity against VHA and sAC.

## Results

Western blotting revealed high abundance of NKA, CA, NKCC, VHA, sAC, and PMCA protein in Pacific Chub Mackerel inner ears (Fig. 1). The immunoreactive bands matched the predicted size of each target protein (NKA-α subunit: ~ 100 kDa with both mono- and polyclonal antibodies; CA: ~ 30 kDa; NKCC: ~ 200 kDa; VHA-b subunit: ~ 55 kDa; PMCA: ~ 140 kDa; sAC: ~ 180, 110, and 50 kDa), were sharp and distinct, and were absent in control blots in which the primary antibody was omitted. No bands were detected in anti-VHA and anti-sAC antibodies' pre-immune and peptide pre-absorption controls.

Next, we examined the expression of these proteins within specific saccular epithelial cells using immunohistochemistry. NKA was abundantly expressed within cells adjacent to the endolymph (Fig. 2a). Higher magnification images revealed NKA immunostaining produced a dense intracellular speckled pattern (Fig. 2b), which indicates NKA is present in the highly infolded basolateral membrane. Double immunolabeling with anti-complex IV antibodies revealed the NKA-rich ionocytes are MR (Fig. 2c) and contain abundant NKCC (Fig. 2d). Furthermore, the resulting “yellow” signal from dual NKA and NKCC immunolabeling indicated

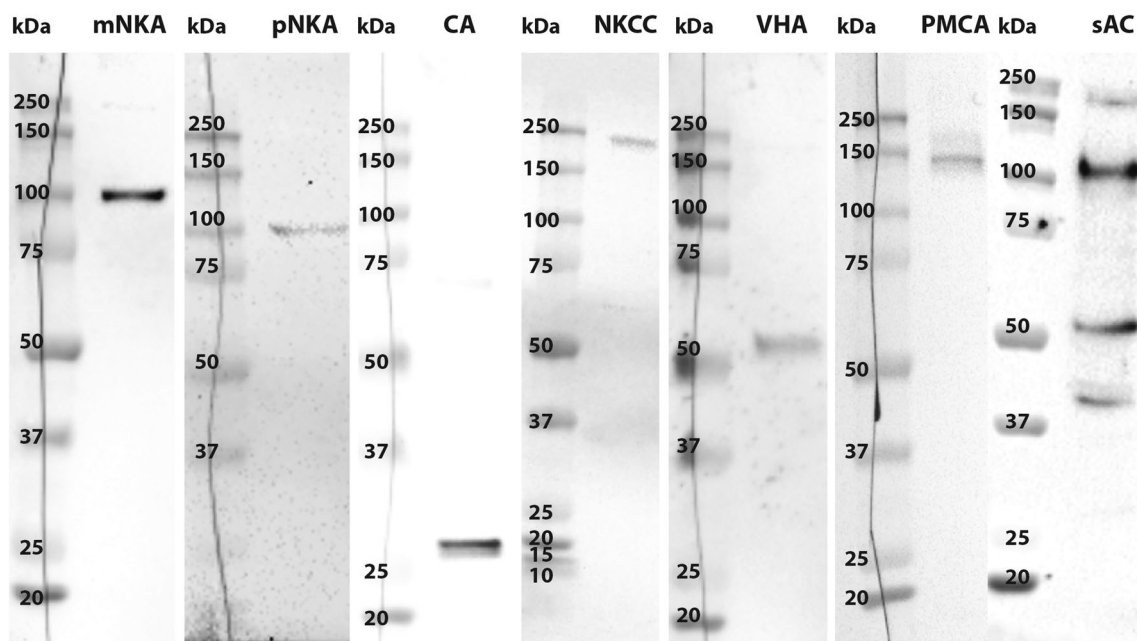
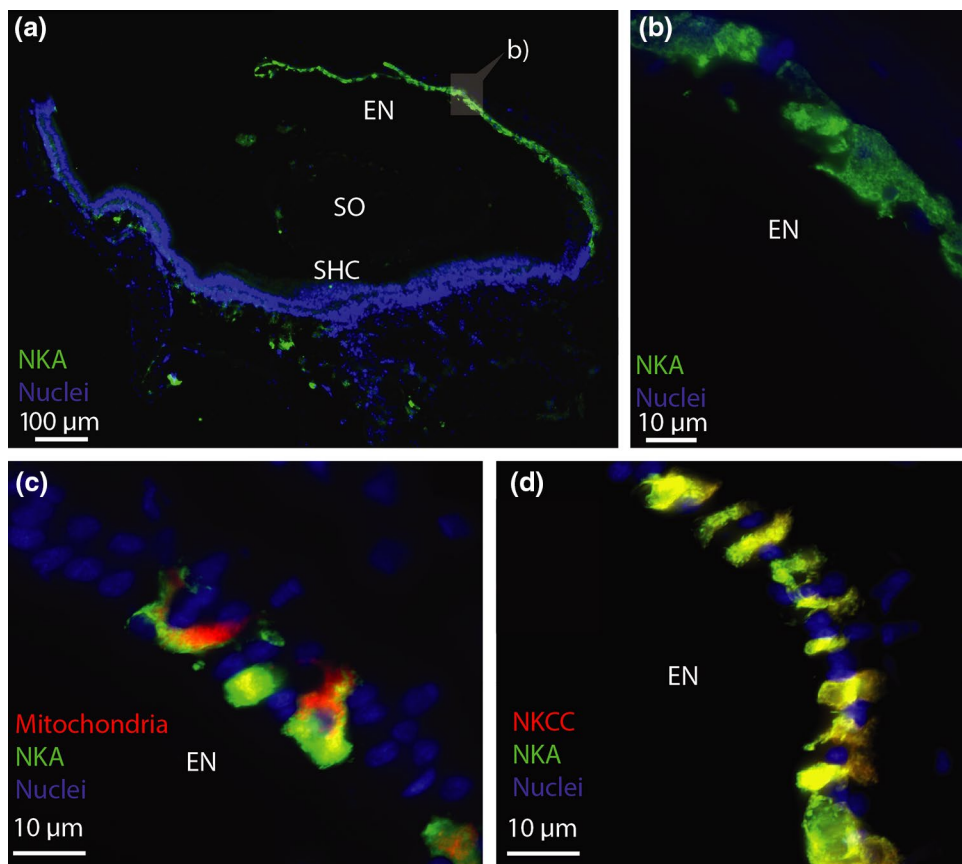


**Fig. 1** Western blot analysis of inner ear homogenates. Antibodies against monoclonal  $\text{Na}^+/\text{K}^+$ -ATPase (mNKA), polyclonal  $\text{Na}^+/\text{K}^+$ -ATPase (pNKA), carbonic anhydrase (CA),  $\text{Na}^+-\text{K}^+-\text{Cl}^-$ -co-transporter (NKCC), V-type  $\text{H}^+$  ATPase (VHA),

plasma membrane calcium ATPase (PMCA), and soluble adenylyl cyclase (sAC) reveal bands matching the predicted size of respective proteins. Molecular marker is shown on the left of each respective blot

**Fig. 2** Characterization of Type-I ionocytes within the saccular epithelium. Histological saggital section immunostained with (a)  $\text{Na}^+/\text{K}^+$ -ATPase (NKA, green). **b** Magnified view of the NKA-rich ionocytes revealed abundant staining in a dense, speckled pattern resembling a developed basolateral infolding. Dual-immunostaining revealed the NKA-rich (green) ionocyte is also (c) mitochondrion-rich (red) and contain abundant (d)  $\text{Na}^+-\text{K}^+-2\text{Cl}^-$ -co-transporter (NKCC, red). Nuclei are stained blue. EN endolymph, SO sagittal otolith protein, SHC sensory hair cell (color figure online)



a strong overlap in the basolateral membrane. CA was also highly expressed in specific saccular epithelial cells; however, double immunolabeling revealed CA was present in cells that were not labeled for NKA (Fig. 3a) or NKCC1 (Fig. 3b). Similarly, double immunolabeling of NKA and VHA (Fig. 4a, b, c) revealed that these two proteins were expressed in different cells. By default, this indicates the CA and VHA were expressed in the same cell type. Overall, these results indicate the presence of two types of ionocytes in the saccular epithelium. “Type-I” ionocytes abundantly express NKA and NKCC1 and are MR, and “Type-II” ionocytes abundantly express CA and VHA.

PMCA was also abundantly expressed in saccular epithelial cells adjacent to the endolymph. The pattern observed following dual immunostaining with NKA indicates PMCA is present in Type-I and Type-II ionocytes (Fig. 5a, b). Unlike NKA and NKCC1 (Fig. 2d), NKA and PMCA

immunofluorescent signals did not overlap significantly (Fig. 5c), suggesting PMCA is predominantly present in cytoplasmic vesicles and not in the basolateral membrane.

In addition, abundant sAC immunolabeling was detected throughout the saccular epithelium (Fig. 5d). Dual immunostaining of sAC and NKA (Fig. 5e, f) and sAC and PMCA (Fig. 5g, h, i) revealed sAC was abundantly expressed in both Type-I and Type-II ionocytes.

Type-I and Type-II ionocytes in the meshwork area were larger than in the patches area (~40  $\mu\text{m}$  vs. ~10  $\mu\text{m}$  wide, respectively; Fig. 4b, c). However, the protein expression profile in each ionocyte type was identical regardless of size. In addition to the previously reported presence of PMCA (Cruz et al. 2009) and VHA (Shiao et al. 2005), we detected NKA (Fig. 2a) and sAC (Fig. 5d) within the sensory hair cells. Unexpectedly, we also observed intense CA (Fig. 6a, b), VHA (Fig. 6c, d), and sAC (Fig. 6e, f) immunoreactivity within the endothelial cells that form the abundant capillaries surrounding the meshwork area.

## Discussion

Here, we characterized two types of ionocytes within the Pacific Chub Mackerel’s saccular epithelium: Type-I ionocytes are MR and express abundant NKA, NKCC1, PMCA, and sAC, whereas Type-II ionocytes express abundant CA, VHA, PMCA, and sAC (Fig. 7). Ionocyte distribution and size patterns were similar to those reported in most previous studies (Mayer-Gostan et al. 1997; Pisam et al. 1998): larger ionocytes bordered the meshwork area, while smaller ionocytes were found in the patches area. However, there were no differences in protein expression between the larger Type-I and Type-II meshwork ionocytes and the smaller Type-I and Type-II patches ionocytes, further supporting the idea that only two types of ionocytes exist within the saccular epithelium. This suggests that the differences in ionic composition between the proximal and distal endolymph are the result of different ion transporting rates in these two regions and not due to the presence of different ion transporting mechanisms. Additional factors that surely contribute to the heterogeneous endolymph ionic composition and otolith calcification rates include the activity of hair cells and the secretion of glycoproteins that promote carbonate precipitation, both taking place in the meshwork area and proximal endolymph (reviewed in Payan et al. 2004; Allemand et al. 2008).

Our results on the marine Pacific Chub Mackerel generally agree with the literature about ion transporting mechanisms in fish inner ear epithelia, which is largely based on research on freshwater fishes. The main differences were the localization of VHA and PMCA. The former was reported to be exclusively expressed in sensory hair cells in the inner ear of Zebrafish embryos (Shiao et al. 2005),

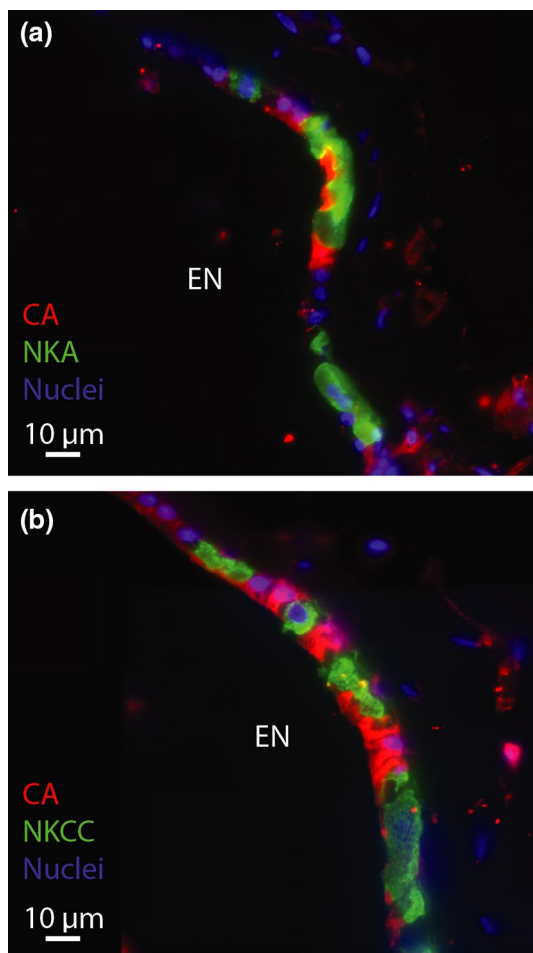
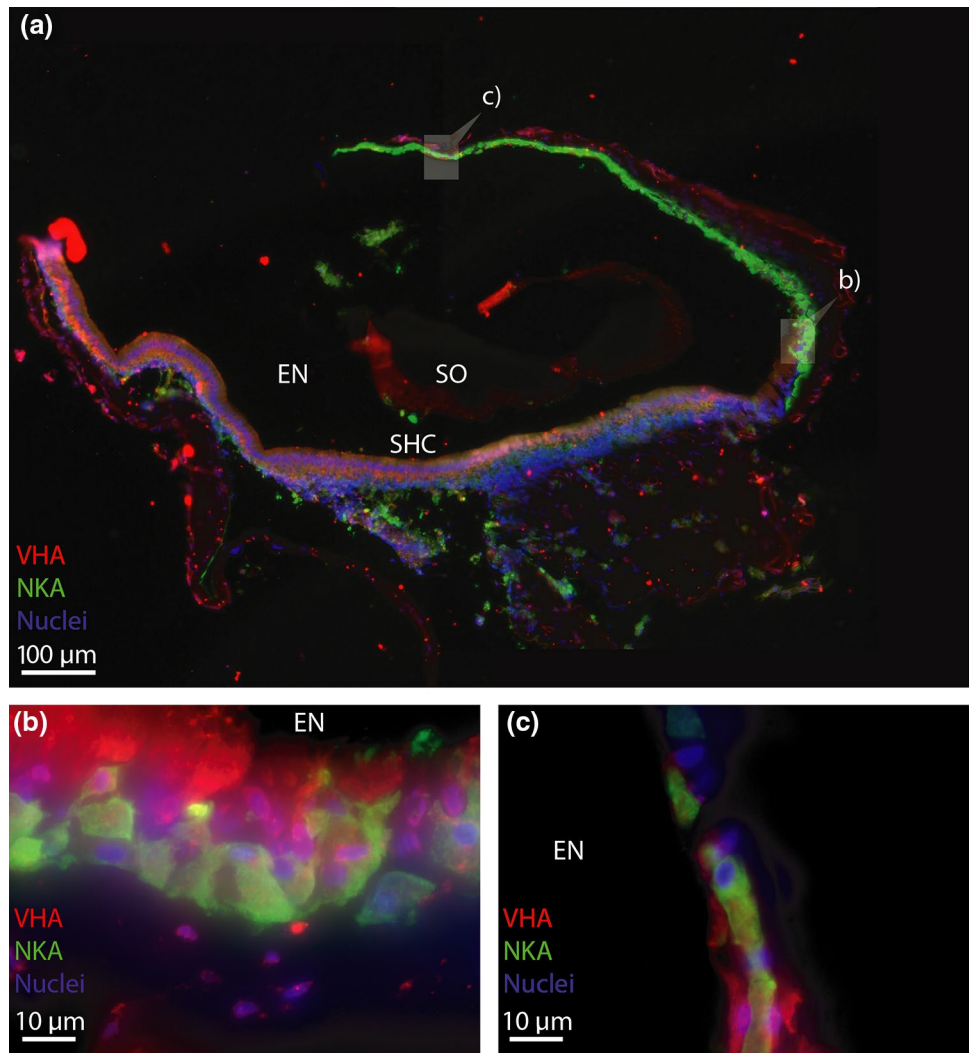


**Fig. 3** Evidence for two types of ionocytes within the saccular epithelium. Dual-immunostaining of ionocytes within the saccular epithelium revealed carbonic anhydrase (CA; red) is expressed in cells that are different from the (a)  $\text{Na}^+/\text{K}^+$ -ATPase (NKA; green) and (b)  $\text{Na}^+/\text{K}^+/\text{2Cl}^-$ -co-transporter (NKCC, green)-rich Type-I ionocyte. Nuclei are stained blue. EN endolymph (color figure online)

**Fig. 4** Characterization of Type-II ionocytes within the saccular epithelium. **a** Histological saggital section immunostained with Na<sup>+</sup>/K<sup>+</sup>-ATPase (NKA, green) and V-type H<sup>+</sup>-ATPase (VHA, red). **b** Higher magnification image of saccular ionocytes of the larger meshwork ionocytes and **(c)** the smaller patches ionocytes indicate NKA-rich and VHA-rich cells are different cells. Nuclei are stained blue. *EN* endolymph; *SO* sagittal otolith protein, *SHC* sensory hair cell (color figure online)



and the latter was only studied at the mRNA level and predominantly found in hair cells as well (Cruz et al. 2009). Future experiments should confirm whether the differences between Pacific Chub Mackerel and Zebrafish are species or life stage-specific, environmentally based (i.e., freshwater vs. seawater), or due to different immunostaining techniques and antibodies.

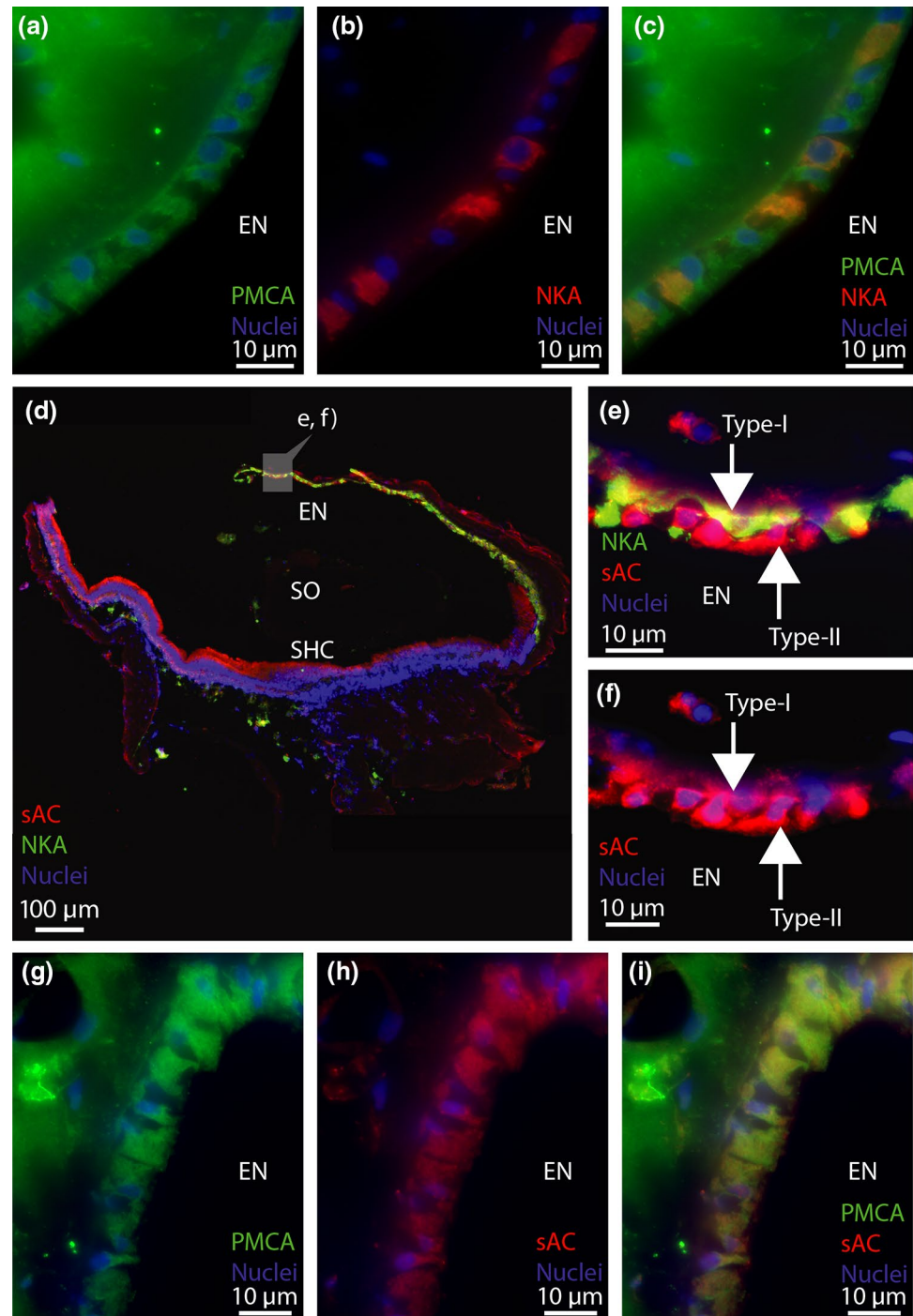
#### Putative functions of fish inner ear epithelial ionocyte function

Based on the presence of NKA and NKCC1, the Type-I ionocytes are likely responsible for secreting K<sup>+</sup> into the endolymph, where it can reach concentrations > 40 fold higher than in blood plasma (Payan et al. 1997, 1999; Ghanem et al. 2008). Given that NKCC1 knockout results in inner ear collapses due to lack of fluid in Zebrafish larvae (Abbas and Whitfield 2009), one of the roles of NKCC1-driven K<sup>+</sup> secretion is to osmotically drive fluid transport.

In addition, the K<sup>+</sup>-rich endolymph is essential for mechanoreception by the sensory hair cells (Zdebek et al. 2009). This model would imply that Type-I ionocytes express K<sup>+</sup> channels in their apical membrane, and should be further investigated in future studies. The outwardly conducting KCNQ1/KCNE1 K<sup>+</sup> channels found on the apical membrane of the analogous “dark” cells of mammalian inner ear are promising candidates (Nicolas et al. 2001).

In contrast, the high abundance of CA and VHA in Type-II ionocytes suggests these cells are involved in promoting otolith calcification by secreting HCO<sub>3</sub><sup>-</sup> into the endolymph and removing H<sup>+</sup>. The CA-catalyzed hydration of CO<sub>2</sub> (for example from the abundant mitochondria from the adjacent Type-I ionocytes) would provide HCO<sub>3</sub><sup>-</sup> to be secreted into the endolymph by yet unidentified apical anion exchangers. The H<sup>+</sup> that is simultaneously produced might be removed by VHA, either into intracellular vesicles as proposed by Mayer-Gostan et al (1997) or upon VHA insertion into the basolateral membrane as reported in the base-secreting

**Fig. 5** Presence of plasma membrane  $\text{Ca}^{2+}$  ATPase and soluble adenylyl cyclase in Type-I and Type-II ionocytes. **(a, b, c)** Dual immunostaining of plasma membrane  $\text{Ca}^{2+}$ -ATPase (PMCA, green) with  $\text{Na}^+/\text{K}^+$ -ATPase (NKA, red). Notice that PMCA is present in all NKA-rich cells (Type-I ionocyte), as well as in adjacent cells without NKA signal (Type-II ionocytes). **d** Histological sagittal section immunostained with soluble adenylyl cyclase (sAC, red) and  $\text{Na}^+/\text{K}^+$ -ATPase (NKA, green). **e, f** Higher magnification images reveal sAC is present in both the NKA-rich Type-I ionocytes (green) and Type-II ionocytes (indicated by ionocytes lacking NKA signal). **g, h, i** The presence of PMCA (green) and sAC (red) in both Type-I and Type-II ionocytes was further conformed by dual-staining. Nuclei are stained blue. *EN* endolymph; *SO* sagittal otolith protein, *SHC* sensory hair cell (color figure online)



cells of elasmobranch gills (Tresguerres et al. 2005; Roa and Tresguerres 2016).

Both Type-I and Type-II ionocytes also expressed PMCA, which has been previously shown to be important for otolith calcification based on the effects of genetic knockdown (Cruz et al. 2009) and pharmacological inhibition of calmodulin-antagonist of PMCA activity (Mugiya and Yoshida 1995). The presence of PMCA throughout the cytoplasm suggests  $\text{Ca}^{2+}$  sequestration in vesicles,

which may be transported to the apical membrane and its contents exocytosed into the calcifying fluid as proposed in coral calcifying cells (Barott et al. 2015b; Barron et al. 2018). Other proposed transcellular pathways for  $\text{Ca}^{2+}$  transport include  $\text{Ca}^{2+}$  channels and  $\text{Na}^+/\text{Ca}^{2+}$  exchangers (Mugiya and Yoshida 1995; Thomas et al. 2019), and the identification of their cellular and subcellular localizations would contribute greatly to the mechanistic model of otolith calcification.

**Fig. 6** Inner ear saccular epithelium capillaries express CA, VHA, and sAC. Histological section dual-stained with (a, b) carbonic anhydrase (CA, red) and Na<sup>+</sup>-K<sup>+</sup>-2Cl<sup>-</sup>-co-transporter (NKCC, green), (c, d) V-type H<sup>+</sup>-ATPase-rich (VHA, green) and Na<sup>+</sup>/K<sup>+</sup>-ATPase (NKA, green), and (e, f) soluble adenylyl cyclase (sAC, red) and NKA (green). Nuclei are stained blue. EN endolymph; CAP capillary (color figure online)

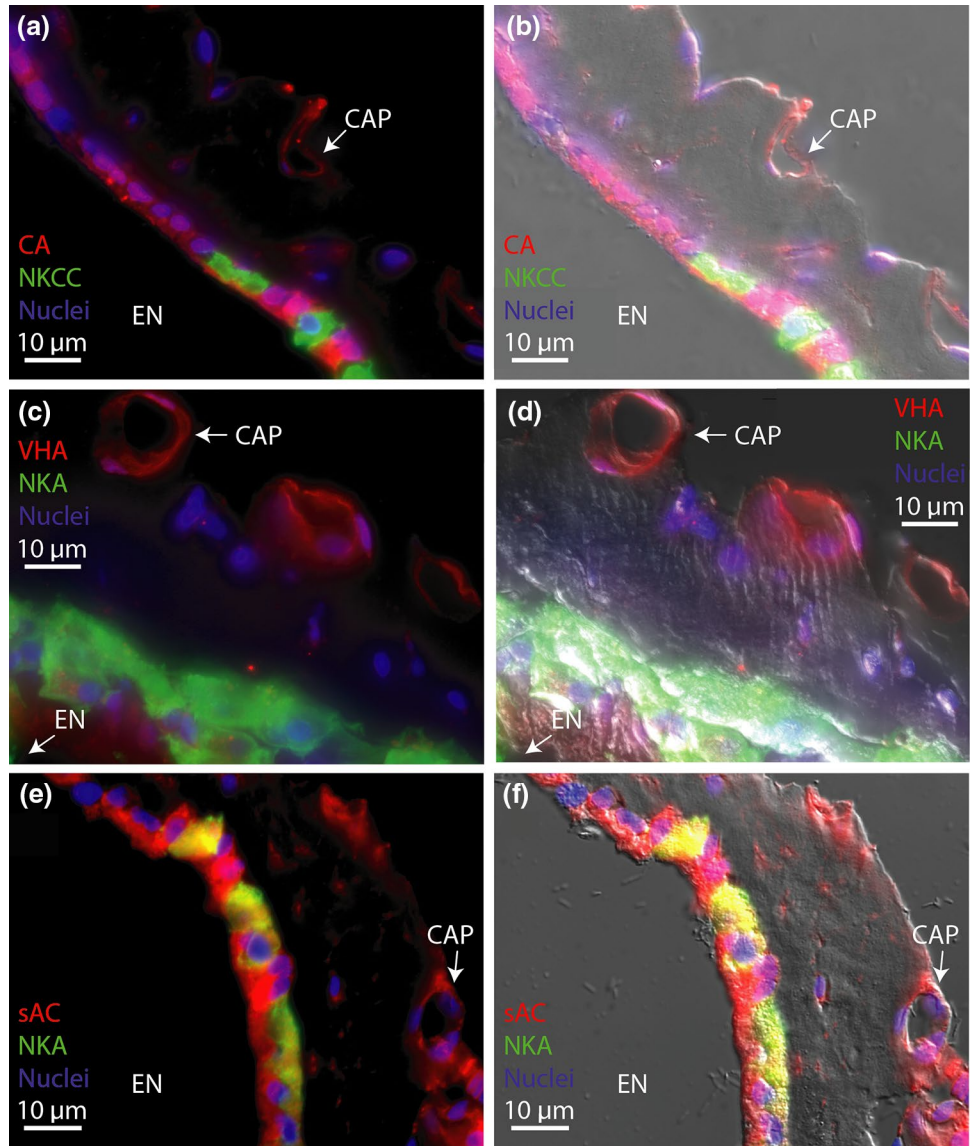
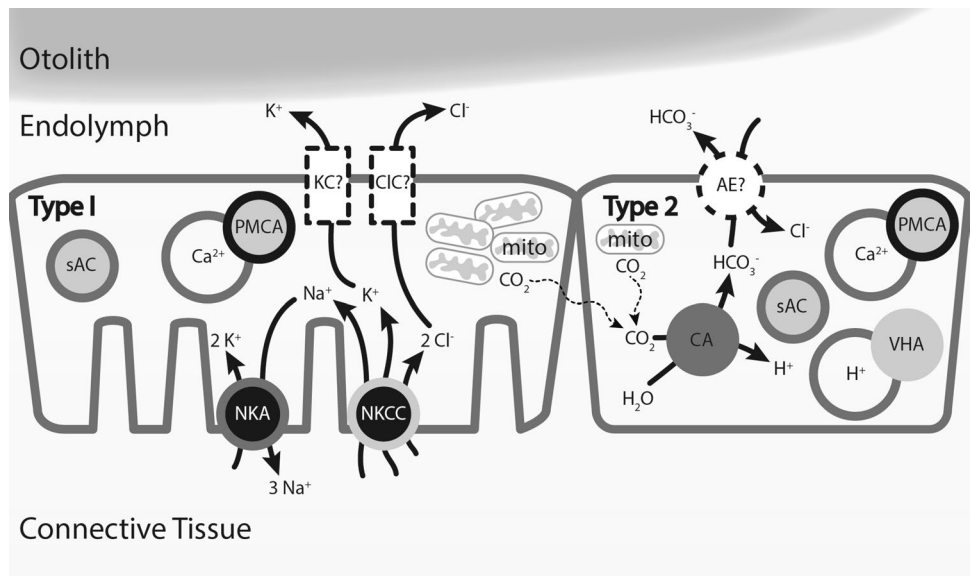


**Fig. 7** Proposed model for otolith calcification by the two types of ionocytes within the inner ear saccular epithelium. NKA Na<sup>+</sup>/K<sup>+</sup>-ATPase, NKCC Na<sup>+</sup>-K<sup>+</sup>-Cl<sup>-</sup>-co-transporter, mito mitochondria, CA carbonic anhydrase, VHA V-type H<sup>+</sup> ATPase, PMCA plasma membrane calcium ATPase, sAC soluble adenylyl cyclase, AE anion exchanger, KC K<sup>+</sup> channel, CIC Cl<sup>-</sup> channel. Capillaries that supply O<sub>2</sub> (and potentially HCO<sub>3</sub><sup>-</sup>) are not shown for simplicity, though they are especially important in the meshwork area. Ion transport is indicated by a solid line, and gas diffusion is indicated by a dashed, squiggly line



## A potential regulatory mechanism of otolith calcification

Both Type-I and Type-II ionocytes contained sAC, an evolutionary conserved acid–base sensing enzyme that produces the messenger molecule cAMP (Chen et al. 2000; Tresguerres, 2014). The effects of plasma and endolymph acid–base status on otolith calcification are well established (Takagi, 2002; Payan et al. 2004; Allemand et al. 2008), and sAC may be one of the underlying signaling mechanisms that senses and regulates the activity of calcification-relevant ion transporting proteins. Supporting this possibility, some of the same ion-transporting proteins found in Type-I and Type-II ionocytes have been shown to be under sAC regulation in many other epithelia. In the intestine of marine teleosts, sAC senses elevations in  $[\text{HCO}_3^-]$  and regulates NKA and NKCC activity to promote luminal carbonate precipitation and fluid transport (Tresguerres et al. 2010b; Carvalho et al. 2012). In marine elasmobranchs gills, sAC senses blood alkalosis and activates VHA -and possibly the apical anion exchanger pendrin- to mediate compensatory  $\text{HCO}_3^-$  secretion and  $\text{H}^+$  absorption (Tresguerres et al. 2010c; Roa et al. 2014; Roa and Tresguerres, 2016). In addition to being directly stimulated by  $\text{HCO}_3^-$ , sAC is stimulated by  $\text{Ca}^{2+}$  (Litvin et al. 2003), providing another potential regulatory mechanism for otolith calcification. Interestingly, sAC is also abundantly expressed in coral calcifying cells (Barott et al. 2017) and in oyster mantle (Barron et al. 2012), suggesting a conserved role in regulating transepithelial ion transport for calcification.

## A novel regulatory role of capillaries in regulating otolith calcification?

The connective tissues surrounding the inner ear contain numerous capillaries, which are especially abundant near the meshwork area (Saitoh 1990; Mayer-Gostan et al. 1997). Unexpectedly, we found the endothelial cells that form such capillaries to abundantly express CA, VHA, and sAC. This is consistent with previous reports of CA within the cytoplasm of capillaries in the analogous mammalian inner ear (Watanabe and Ogawa 1984). We tentatively propose that the activities of these proteins are relevant for otolith calcification by mediating the transport of  $\text{CO}_2/\text{HCO}_3^-$  from the blood to the endolymph, and by facilitating the removal of excess  $\text{H}^+$  generated as a result of  $\text{CaCO}_3$  precipitation. In addition, the local acidification of the capillary lumen could trigger the Root effect in circulating red blood cells, thus promoting  $\text{O}_2$  offloading to sustain aerobic metabolism of ionocytes and sensory hair cells within the saccular epithelium. Such a mechanism was originally described in fish swim bladder and eye (reviewed in Pelster 2001), and more recently proposed to apply more broadly to other

highly aerobic fish tissues including the eye (Fairbanks et al. 1969), muscle (Rummer et al. 2013), and intestine (Cooper et al. 2014).

## Conclusions, future directions and significance

Our proposed model is consistent with previous functional studies conducted on isolated fish inner ear organ that suggested the involvement of NKA, CA, and PMCA (as well as  $\text{Na}^+/\text{Ca}^{2+}$  exchanger,  $\text{Ca}^{2+}$  channels, and  $\text{Na}^+/\text{H}^+$  exchanger) based on acid–base titration and  $^{45}\text{Ca}^{2+}$  incorporation experiments in combination with pharmacological inhibitors (Mugiya and Yoshida 1995; Payan et al. 1997). Furthermore, functional evidence for the roles of NKCC1 (Abbas and Whitfield 2009) and PMCA (Cruz et al. 2009) is available through the genetic downregulation experiments on Zebrafish larvae mentioned above. More recently, the presence of many of those proteins as well as VHA has been confirmed through an extensive proteomic and transcriptomic survey (Thomas et al. 2019) (with the caveat that analyses were conducted on samples that contain both inner ear and brain tissue). Our results expand and complement those previous studies by establishing the transporter's cellular and subcellular localization, ultimately leading to the identification of two types of ionocytes. In addition, our results revealed sAC is present in both types of ionocytes, providing a potential mechanism that can regulate otolith calcification in response to acid–base variations. Ongoing efforts in our laboratory are attempting to functionally characterize the putative regulatory role of sAC on inner ear function; however, sAC's presence within both types of ionocytes, sensory hair cells, and capillaries is a significant hurdle for studies at the organ and whole organism level. For example, putative changes in protein or mRNA abundance in ionocytes in response to experimental manipulations would be confounded by the background provided by all the other cell types in the tissue, which are the majority. Thus, detailed functional studies on the underlying ion transport mechanism would require the development of ionocyte primary cultures. Similar considerations apply to efforts to elucidating the functional roles of CA, VHA, and sAC in the capillaries near the meshwork area.

The inner ear organ allows fish to sense and respond to its environment and, therefore, is essential for survival. In addition, analyses on otolith rings provide valuable information regarding daily and seasonal growth bands, trace element signatures (Swearer et al. 1999), exposure to environmental salinity and temperature (Campana 1999; Elsdon and Gilanders 2002), and diet (Radtke et al. 1996; Nelson et al. 2011; von Biela et al. 2015). Thus, in addition to its intrinsic value from physiological and evolutionary perspectives, information about the cellular mechanisms underlying otolith calcification can improve current fisheries assessment

tools and help predict the effects of environmental stressors, and in particular ocean acidification, on otolith growth and function from a mechanistic perspective.

**Acknowledgements** GTK was supported by the National Science Foundation (NSF) Graduate Research Fellowship Program and the NSF Graduate Research Internship Program. This research was supported by grant NSF IOS #1754994 to M.T. We thank Jake Munich for his assistance in capturing Pacific Chub Mackerel. The authors would like to thank the two anonymous reviewers for their helpful comments.

## References

- Abbas L, Whitfield TT (2009) Nkcc1 (Slc12a2) is required for the regulation of endolymph volume in the otic vesicle and swim bladder volume in the zebrafish larva. *Development* 136:2837–2848. <https://doi.org/10.1242/dev.034215>
- Allemand D, Mayer-Gostan N, De Pontual H, Boeuf G, Payan P (2008) Fish otolith calcification in relation to endolymph chemistry. *Handb Biominer Biol Asp Struct Form* 1:291–308. <https://doi.org/10.1002/9783527619443.ch17>
- Allmon EB, Esbaugh AJ (2017) Carbon dioxide induced plasticity of branchial acid-base pathways in an estuarine teleost. *Sci Rep* 7:45680. <https://doi.org/10.1038/srep45680>
- Barott K, Venn AA, Perez SO, Tambuttè S, Tresguerres M (2015a) Coral host cells acidify symbiotic algal microenvironment to promote photosynthesis. *Proc Natl Acad Sci U S A* 112:607–612. <https://doi.org/10.1073/pnas.1413483112>
- Barott KL, Perez SO, Linsmayer LB, Tresguerres M (2015b) Differential localization of ion transporters suggests distinct cellular mechanisms for calcification and photosynthesis between two coral species. *Am J Physiol Regul Integr Comp Physiol* 309:R235–R246. <https://doi.org/10.1152/ajpregu.00052.2015>
- Barott KL, Barron ME, Tresguerres M (2017) Identification of a molecular pH sensor in coral. *Proc R Soc B Biol Sci* 284:20171769. <https://doi.org/10.1098/rspb.2017.1769>
- Barron ME, Roa JNBR, Tresguerres M (2012) Pacific oyster mantle, gill and hemocytes express the bicarbonate-sensing enzyme soluble adenylyl cyclase. *FASEB J* 26:1070–1072
- Barron ME, Thies AB, Espinoza JA, Barott KL, Hamdoun A, Tresguerres M (2018) A vesicular Na<sup>+</sup>/Ca<sup>2+</sup> exchanger in coral calcifying cells. *PLoS ONE* 13:e0205367. <https://doi.org/10.1371/journal.pone.0205367>
- Beier M, Anken R, Hilbig R (2006) Sites of calcium uptake of fish otoliths correspond with macular regions rich of carbonic anhydrase. *Adv Space Res* 38:1123–1127. <https://doi.org/10.1016/j.asr.2005.10.042>
- Bignami S, Enochs IC, Manzello DP, Sponaugle S, Cowen RK (2013) Ocean acidification alters the otoliths of a pantropical fish species with implications for sensory function. *Proc Natl Acad Sci* 110:7366–7370. <https://doi.org/10.1073/pnas.1301365110>
- Borelli G, Guibolini ME, Mayer-Gostan N, Priouzeau F, De Pontual H, Allemand D et al (2003) Daily variations of endolymph composition: relationship with the otolith calcification process in trout. *J Exp Biol* 206:2685–2692. <https://doi.org/10.1242/jeb.00479>
- Bradford MM (1976) A rapid and sensitive method for the quantitation of microgram quantities of protein utilizing the principle of protein-dye binding. *Anal Biochem* 72:248–254. [https://doi.org/10.1016/0003-2697\(76\)90527-3](https://doi.org/10.1016/0003-2697(76)90527-3)
- Campana S (1999) Chemistry and composition of fish otoliths: pathways, mechanisms and applications. *Mar Ecol Prog Ser* 188:263–297. <https://doi.org/10.3354/meps188263>
- Campana SE, Neilson JD (1985) Microstructure of fish otoliths. *Can J Fish Aquat Sci* 42:1014–1032
- Carvalho ESM, Gregório SF, Power DM, Canário AVM, Fuentes J (2012) Water absorption and bicarbonate secretion in the intestine of the sea bream are regulated by transmembrane and soluble adenylyl cyclase stimulation. *J Comp Physiol B Biochem Syst Environ Physiol* 182:1069–1080. <https://doi.org/10.1007/s00360-012-0685-4>
- Checkley DM, Dickson AG, Takahashi M, Radich JA, Eisenkolb N, Asch R (2009) Elevated CO<sub>2</sub> enhances otolith growth in young fish. *Science* 324:1683. <https://doi.org/10.1126/science.1169806>
- Chen Y, Cann MJ, Litvin TN, Iourgenko V, Sinclair ML, Levin LR et al (2000) Soluble adenylyl cyclase as an evolutionarily conserved bicarbonate sensor. *Science* 289:625–628. <https://doi.org/10.1126/science.289.5479.625>
- Cooper CA, Regan MD, Brauner CJ, De Bastos ESR, Wilson RW (2014) Osmoregulatory bicarbonate secretion exploits H<sup>+</sup>-sensitive haemoglobins to autoregulate intestinal O<sub>2</sub> delivery in euryhaline teleosts. *J Comp Physiol B Biochem Syst Environ Physiol* 184:865–876. <https://doi.org/10.1007/s00360-014-0844-x>
- Cruz S, Shiao JC, Liao BK, Huang CJ, Hwang PP (2009) Plasma membrane calcium ATPase required for semicircular canal formation and otolith growth in the zebrafish inner ear. *J Exp Biol* 212:639–647. <https://doi.org/10.1242/jeb.022798>
- Dijkgraaf S (1960) Hearing in bony fishes. *Proc R Soc B* 152:51–54
- Elsdon TS, Gillanders BM (2002) Interactive effects of temperature and salinity on otolith chemistry: challenges for determining environmental histories of fish. *Can J Fish Aquat Sci* 59:1796–1808. <https://doi.org/10.1139/f02-154>
- Esbaugh AJ, Cutler B (2016) Intestinal Na<sup>+</sup>, K<sup>+</sup>, 2Cl<sup>-</sup>-cotransporter 2 plays a crucial role in hyperosmotic transitions of a euryhaline teleost. *Physiol Rep* 4:1–12. <https://doi.org/10.14814/phy2.13028>
- Esbaugh AJ, Heuer R, Grosell M (2012) Impacts of ocean acidification on respiratory gas exchange and acid-base balance in a marine teleost, *Opsanus beta*. *J Comp Physiol B Biochem Syst Environ Physiol* 182:921–934. <https://doi.org/10.1007/s00360-012-0668-5>
- Esbaugh AJ, Ern R, Nordi WM, Johnson AS (2016) Respiratory plasticity is insufficient to alleviate blood acid–base disturbances after acclimation to ocean acidification in the estuarine red drum, *Sciaenops ocellatus*. *J Comp Physiol B Biochem Syst Environ Physiol* 186:97–109. <https://doi.org/10.1007/s00360-015-0940-6>
- Fairbanks MB, Hoffert JR, Fromm PO (1969) The dependence of the oxygen-concentrating mechanism of the teleost eye (*Salmo gairdneri*) on the enzyme carbonic anhydrase. *J Gen Physiol* 54:203–211. <https://doi.org/10.1085/jgp.54.2.203>
- Furukawa T, Ishii Y (1967) Neurophysiological studies on hearing in goldfish. *J Neurophysiol* 30:1377–1403
- Georgalis T, Gilmour KM, Yorston J, Perry SF (2006) Roles of cytosolic and membrane-bound carbonic anhydrase in renal control of acid-base balance in rainbow trout, *Oncorhynchus mykiss*. *Am J Physiol* 291:407–421. <https://doi.org/10.1152/ajprenal.00328.2005>
- Ghanem TA, Breneman KD, Rabbitt RD, Brown HM (2008) Ionic composition of endolymph and perilymph in the inner ear of the oyster toadfish, *Opsanus tau*. *Biol Bull* 214:83–90. <https://doi.org/10.2307/25066662>
- Hiroi J, Yasumasu S, McCormick SD, Hwang P-P, Kaneko T (2008) Evidence for an apical Na–Cl cotransporter involved in ion uptake in a teleost fish. *J Exp Biol* 211:2584–2599. <https://doi.org/10.1242/jeb.018663>
- Ibsch M, Anken R, Beier M, Rahmann H (2004) Endolymphatic calcium supply for fish otolith growth takes place via the proximal portion of the otocyst. *Cell Tissue Res* 317:333–336. <https://doi.org/10.1007/s00441-004-0930-6>
- Inokuchi M, Hiroi J, Watanabe S, Lee KM, Kaneko T (2008) Gene expression and morphological localization of NHE3, NCC and

- NKCC1a in branchial mitochondria-rich cells of Mozambique tilapia (*Oreochromis mossambicus*) acclimated to a wide range of salinities. *Comp Biochem Physiol A: Mol Integr Physiol* 151:151–158. <https://doi.org/10.1016/j.cbpa.2008.06.012>
- Kwan GT, Wexler JB, Wegner NC, Tresguerres M (2019) Ontogenetic changes in cutaneous and branchial ionocytes and morphology in yellowfin tuna (*Thunnus albacares*) larvae. *J Comp Physiol B Biochem Syst Environ Physiol* 189:81–95. <https://doi.org/10.1007/s00360-018-1187-9>
- Ladich F, Schulz-Mirbach T (2016) Diversity in fish auditory systems: one of the riddles of sensory biology. *Front Ecol Evol* 4:1–26. <https://doi.org/10.3389/fevo.2016.00028>
- Lebovitz RM, Takeyasu K, Fambrough DM (1989) Molecular characterization and expression of the (Na<sup>+</sup> + K<sup>+</sup>)-ATPase alpha-subunit in *Drosophila melanogaster*. *EMBO J* 8:193–202
- Litvin TN, Kamenetsky M, Zarifyan A, Buck J, Levin LR (2003) Kinetic properties of “soluble” adenylyl cyclase: synergism between calcium and bicarbonate. *J Biol Chem* 278:15922–15926. <https://doi.org/10.1074/jbc.M212475200>
- Lytle C, Xu JC, Biemesderfer D, Forbush B (1995) Distribution and diversity of Na–K–Cl cotransport proteins: a study with monoclonal antibodies. *Am J Physiol* 269:C1496–C1505
- Maneja RH, Frommel AY, Geffen AJ, Folkvord A, Piatkowski U, Chang MY et al (2013) Effects of ocean acidification on the calcification of otoliths of larval Atlantic cod *Gadus morhua*. *Mar Ecol Prog Ser* 477:251–258. <https://doi.org/10.3354/meps10146>
- Mayer-Gostan N, Kossmann H, Watrin A, Payan P, Boeuf G (1997) Distribution of ionocytes in the saccular epithelium of the inner ear of two teleosts (*Oncorhynchus mykiss* and *Scophthalmus maximus*). *Cell Tissue Res* 289:53–61. <https://doi.org/10.1007/s004410050851>
- Michael K, Kreiss CM, Hu MY, Koschnick N, Bickmeyer U, Dupont S et al (2016) Adjustments of molecular key components of branchial ion and pH regulation in Atlantic cod (*Gadus morhua*) in response to ocean acidification and warming. *Comp Biochem Physiol Part B* 193:33–46. <https://doi.org/10.1016/j.cbpb.2015.12.006>
- Mugiya Y, Yoshida M (1995) Effects of calcium antagonists and other metabolic on in vitro calcium deposition on otoliths rainbow trout *Oncorhynchus mykiss* modulators. *Fish* 61:1026–1030
- Munday PL, Hernaman V, Dixon DL, Thorrold SR (2011) Effect of ocean acidification on otolith development in larvae of a tropical marine fish. *Biogeosciences* 8:1631–1641. <https://doi.org/10.5194/bg-8-1631-2011>
- Murayama E, Takagi Y, Ohira T, Davis JG, Greene MI, Nagasawa H (2002) Fish otolith contains a unique structural protein, otolin-1. *Eur J Biochem* 269:688–696. <https://doi.org/10.1046/j.0014-2956.2001.02701.x>
- Nelson J, Hanson CW, Koenig C, Chanton J (2011) Influence of diet on stable carbon isotope composition in otoliths of juvenile red drum *Sciaenops ocellatus*. *Aquat Biol* 13:89–95. <https://doi.org/10.3354/ab00354>
- Nicolas M-T, Demêmes D, Martin A, Kupersmidt S, Barhanin J (2001) KCNQ1/KCNE1 potassium channels in mammalian vestibular dark cells. *Hear Res* 153:132–145. [https://doi.org/10.1016/S0378-5955\(00\)00268-9](https://doi.org/10.1016/S0378-5955(00)00268-9)
- Pannella G (1971) Fish otoliths: daily growth layers and periodical patterns. *Science* 173:1124–1127
- Payan P, Kossmann H, Watrin A, Mayer-Gostan N, Boeuf G (1997) Ionic composition of endolymph in teleosts: origin and importance of endolymph alkalinity. *J Exp Biol* 200:1905–1912
- Payan P, Edeyer A, de Pontual H, Borelli G, Boeuf G, Mayer-Gostan N (1999) Chemical composition of saccular endolymph and otolith in fish inner ear: lack of spatial uniformity. *Am J Physiol* 277:R123–R131
- Payan P, Borelli G, Priouzeau F, De Pontual H, Boeuf G, Mayer-Gostan N (2002) Otolith growth in trout *Oncorhynchus mykiss*: supply of Ca<sup>2+</sup> and Sr<sup>2+</sup> to the saccular endolymph. *J Exp Biol* 205:2687–2695
- Payan P, De Pontual H, Boeuf G, Mayer-Gostan N (2004) Endolymph chemistry and otolith growth in fish. *CR Palevol* 3:535–547. <https://doi.org/10.1016/j.crpv.2004.07.013>
- Pelster B (2001) The generation of hyperbaric oxygen tensions in fish. *Physiology* 16:287–291. <https://doi.org/10.1152/physiologyonline.2001.16.6.287>
- Pimentel MS, Faleiro F, Dionisio G, Repolho T, Pousao-Ferreira P, Machado J et al (2014) Defective skeletogenesis and oversized otoliths in fish early stages in a changing ocean. *J Exp Biol* 217:2062–2070. <https://doi.org/10.1242/jeb.092635>
- Pisam M, Payan P, LeMoal C, Edeyer A, Boeuf G, Mayer-Gostan N (1998) Ultrastructural study of the saccular epithelium of the inner ear of two teleosts, *Oncorhynchus mykiss* and *Psetta maxima*. *Cell Tissue Res* 294:261–270. <https://doi.org/10.1007/s004410051176>
- Qin Z, Lewis JE, Perry SF (2010) Zebrafish (*Danio rerio*) gill neuroepithelial cells are sensitive chemoreceptors for environmental CO<sub>2</sub>. *J Physiol* 588:861–872. <https://doi.org/10.1113/jphysiol.2009.184739>
- Radtke RL, Lenz P, Showers W, Moksness E (1996) Environmental information stored in otoliths: insights from stable isotopes. *Mar Biol* 127:161–170. <https://doi.org/10.1007/BF00993656>
- Roa JN, Tresguerres M (2016) Soluble adenylyl cyclase is an acid-base sensor in epithelial base-secreting cells. *Am J Physiol Cell Physiol* 311:C340–C349. <https://doi.org/10.1152/ajpcell.00089.2016>
- Roa JN, Tresguerres M (2017) Bicarbonate-sensing soluble adenylyl cyclase is present in the cell cytoplasm and nucleus of multiple shark tissues. *Physiol Rep* 5:e13090. <https://doi.org/10.14814/phy2.13090>
- Roa JN, Munévar CL, Tresguerres M (2014) Feeding induces translocation of vacuolar proton ATPase and pendrin to the membrane of leopard shark (*Triakis semifasciata*) mitochondrion-rich gill cells. *Comp Biochem Physiol Part A Mol Integr Physiol* 174:29–37. <https://doi.org/10.1016/j.cbpa.2014.04.003>
- Rummer JL, McKenzie DJ, Innocenti A, Supuran CT, Brauner CJ (2013) Root effect hemoglobin may have evolved to enhance general tissue oxygen delivery. *Science* 340:1327–1329. <https://doi.org/10.1126/science.1233692>
- Saitoh S (1990) Localization and ultrastructure of mitochondria-rich cells in the inner ears of goldfish and tilapia. *J Ichthyology* 37:49–55
- Schade FM, Clemmesen C, Mathias Wegner K (2014) Within- and transgenerational effects of ocean acidification on life history of marine three-spined stickleback (*Gasterosteus aculeatus*). *Mar Biol* 161:1667–1676. <https://doi.org/10.1007/s00227-014-2450-6>
- Shen SG, Chen F, Schoppik DE, Checkley DM (2016) Otolith size and the vestibulo-ocular reflex of larvae of white seabass *Atractoscion nobilis* at high pCO<sub>2</sub>. *Mar Ecol Prog Ser* 553:173–182. <https://doi.org/10.3354/meps11791>
- Shiao JC, Lin LY, Horng JL, Hwang PP, Kaneko T (2005) How can teleostean inner ear hair cells maintain the proper association with the accreting otolith? *J Comp Neurol* 488:331–341. <https://doi.org/10.1002/cne.20578>
- Swearer SE, Caselle JE, Lea DW, Warner RR (1999) Larval retention and recruitment in an island population of a coral-reef fish. *Nature* 402:799–802. <https://doi.org/10.1038/45533>
- Takagi Y (1997) Meshwork arrangement of mitochondria-rich, Na<sup>+</sup>, K<sup>+</sup>-ATPase-rich cells in the saccular epithelium of rainbow trout (*Oncorhynchus mykiss*) inner ear. *Anat Rec* 248:483–489. [https://doi.org/10.1002/\(SICI\)1097-0185\(199708\)248:4%3c483::AID-AR1%3e3.0.CO;2-N](https://doi.org/10.1002/(SICI)1097-0185(199708)248:4%3c483::AID-AR1%3e3.0.CO;2-N)
- Takagi Y (2002) Otolith formation and endolymph chemistry: a strong correlation between the aragonite saturation state and pH in the

- endolymph of the trout otolith organ. *Mar Ecol Prog Ser* 231:237–245. <https://doi.org/10.3354/meps231237>
- Thomas ORB, Swearer SE, Kapp EA, Peng P, Tonkin-Hill GQ, Papenfuss A et al (2019) The inner ear proteome of fish. *FEBS J* 286:66–81. <https://doi.org/10.1111/febs.14715>
- Tohse H, Mugiya Y (2001) Effects of enzyme and anion transport inhibitor on in vitro incorporation of inorganic carbon and calcium into endolymph and otoliths in salmon *Oncorhynchus masou*. *Comp Biochem Physiol A Mol Integr Physiol* 128:177–184
- Tohse H, Mugiya Y (2008) Sources of otolith carbonate: experimental determination of carbon incorporation rates from water and metabolic CO<sub>2</sub>, and their diel variations. *Aquat Biol* 1:259–268. <https://doi.org/10.3354/ab00029>
- Tohse H, Ando H, Mugiya Y (2004) Biochemical properties and immunohistochemical localization of carbonic anhydrase in the sacculus of the inner ear in the salmon *Oncorhynchus masou*. *Comp Biochem Physiol A Mol Integr Physiol* 137:87–94. [https://doi.org/10.1016/S1095-6433\(03\)00272-1](https://doi.org/10.1016/S1095-6433(03)00272-1)
- Tohse H, Murayama E, Ohira T, Takagi Y, Nagasawa H (2006) Localization and diurnal variations of carbonic anhydrase mRNA expression in the inner ear of the rainbow trout *Oncorhynchus mykiss*. *Comp Biochem Physiol B Biochem Mol Biol* 145:257–264. <https://doi.org/10.1016/j.cbpb.2006.06.011>
- Tresguerres M (2014) sAC from aquatic organisms as a model to study the evolution of acid/base sensing. *Biochim Biophys Acta Mol Basis Dis* 1842:2629–2635. <https://doi.org/10.1016/j.bbadi.2014.06.021>
- Tresguerres M, Katoh F, Fenton H, Jasinska E, Goss GG (2005) Regulation of branchial V-H(+)-ATPase, Na(+)/K(+)-ATPase and NHE2 in response to acid and base infusions in the Pacific spiny dogfish (*Squalus acanthias*). *J Exp Biol* 208:345–354. <https://doi.org/10.1242/jeb.01382>
- Tresguerres M, Buck J, Levin LR (2010a) Physiological carbon dioxide, bicarbonate, and pH sensing. *Pflugers Arch Eur J Physiol* 460:953–964. <https://doi.org/10.1007/s00424-010-0865-6>
- Tresguerres M, Levin LR, Buck J, Grosell M (2010b) Modulation of NaCl absorption by [HCO<sub>3</sub><sup>-</sup>] in the marine teleost intestine is mediated by soluble adenylyl cyclase. *AJP Regul Integr Comp Physiol* 299:R62–R71. <https://doi.org/10.1152/ajpregu.00761.2009>
- Tresguerres M, Parks SK, Salazar E, Levin LR, Goss GG, Buck J (2010c) Bicarbonate-sensing soluble adenylyl cyclase is an essential sensor for acid/base homeostasis. *Proc Natl Acad Sci USA* 107:442–447. <https://doi.org/10.1073/pnas.0911790107>
- von Biela V, Newsome S, Zimmerman C (2015) Examining the utility of bulk otolith δ<sup>13</sup>C to describe diet in wild-caught black rockfish *Sebastes melanops*. *Aquat Biol* 23:201–208. <https://doi.org/10.3354/ab00621>
- Watanabe K, Ogawa A (1984) Carbonic anhydrase activity in stria vascularis and dark cells in vestibular labyrinth. *Ann Otol Rhinol Laryngol* 93:262–266. <https://doi.org/10.1177/000348948409300315>
- Wilson JM, Randall DJ, Donowitz M, Vogl AW, Ip AK (2000) Immunolocalization of ion-transport proteins to branchial epithelium mitochondria-rich cells in the mudskipper (*Periophthalmodon schlosseri*). *J Exp Biol* 203:2297–2310
- Wilson JM, Whiteley NM, Randall DJ (2002) Ionoregulatory changes in the gill epithelia of coho salmon during seawater acclimation. *Physiol Biochem Zool* 75:237–249. <https://doi.org/10.1086/341817>
- Zdebik AA, Wangemann P, Jentsch TJ (2009) Potassium ion movement in the inner ear: Insights from genetic disease and mouse models. *Physiology* 24:307–316. <https://doi.org/10.1152/physiol.00018.2009>

**Publisher's Note** Springer Nature remains neutral with regard to jurisdictional claims in published maps and institutional affiliations.